

High Frequency Transistor Models for Low Noise Applications

Manfred Berroth, Andreas Pascht, Dirk Wiegner
Institute of Electrical and Optical Communication Engineering
University of Stuttgart
Pfaffenwaldring 47
70550 Stuttgart, Germany

Abstract

Mobile communication is one of the fastest growing markets and demands a significant part of the integrated circuit sales. In the past transceivers in the GHz range have required silicon bipolar transistors or even GaAs devices. With the scaling of CMOS technology commercial fabrication lines offer n-channel MOSFET devices with a transit frequency beyond 20 GHz for very large scale integrated circuits. This paper compares the high frequency characteristics of the MOSFET with the SiGe heterostructure bipolar transistor and the GaAs based HEMT for low noise applications.

I. Introduction

The spectacular popularity of mobile telephones drives the demand for low cost and highly integrated circuits also for the radio frequency (RF) transmitter and receiver. This RF frontend is still using tuned circuits with discrete filters and a low level of integration. With regard to costs and integration density complementary metal oxide semiconductor (CMOS) is the technology of choice to permit a free mixture of analog and digital functions. Therefore great interest exists in RF CMOS device characterisation as well as circuit design. Individual wireless building blocks like low noise amplifier, mixer or power amplifier can be fabricated with superior performance using other technologies like silicon bipolar (BJT), heterostructure bipolar transistor (HBT) or GaAs metal semiconductor field effect transistors (MESFET). The object of this article is to compare the MOSFET RF characteristics in regard to noise with a SiGe HBT and a GaAs pseudomorphic high electron mobility transistor (HEMT).

II. High Frequency Noise Model of HEMT

The high frequency noise mechanism of FETs was first calculated by van der Ziel [1] using a gate and drain current noise source $\overline{i_g^2}$ and $\overline{i_d^2}$, and their correlation function $\overline{i_g i_d^*}$. More recently, Pospieszalski [2] proposed an alternative high-frequency noise model neglecting any correlation between the input voltage noise source and drain current noise source. The well-known small-signal equivalent circuit of the FET is used in the common source connection. Therefore we used for all three transistors their small-signal equivalent circuit model with the element values of the operating point and all resistive elements exhibit a noise contribution determined by the physical temperature of the device. This two port noise representation is applied to the MOSFET as well as the HEMT with the findings of [2] and [3], that the input voltage noise source is equivalent to the thermal noise of the real part of the input admittance. The only additional noise source for the field effect transistors is caused by the diffusion noise of the channel current and related to the voltage controlled current source. The small-signal equivalent circuit model of [2], which was extended for large signal applications in [4], is used for the HEMT as shown in Fig. 1 with the adequate noise sources. The excellent agreement of measured and simulated noise parameters using this temperature noise model was reported by several authors e.g. [2], [3], [5].

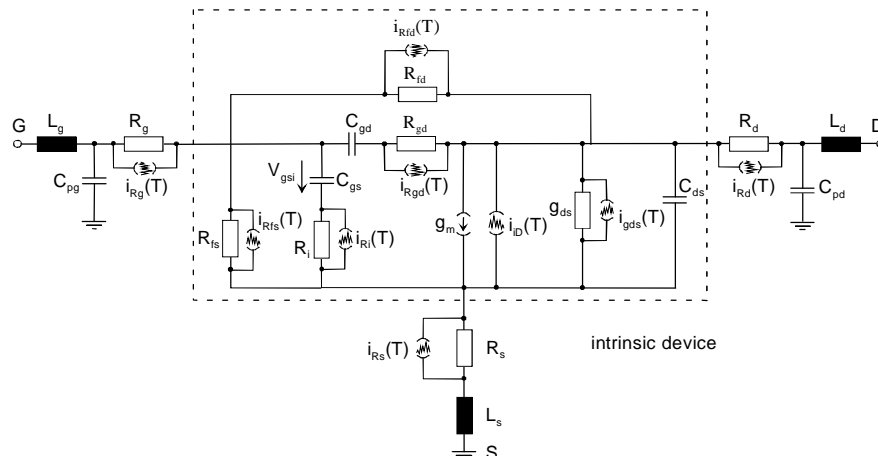


Fig. 1: Noise equivalent circuit model of the HEMT.

III. High Frequency Noise Models of MOSFET

In contrast to the MESFET and HEMT devices, the MOSFET has an isolated gate instead of a Schottky diode. Therefore the differential resistances in the gate-to-source and gate-to-drain lines can be neglected to simplify the small-signal equivalent circuit. The losses of the silicon substrate have to be taken into account by the additional resistances R_{pg} and R_{pd} in series connected with the pad capacitances C_{pg} and C_{pd} respectively. The noise equivalent circuit model for the MOSFET is shown in Fig. 2.

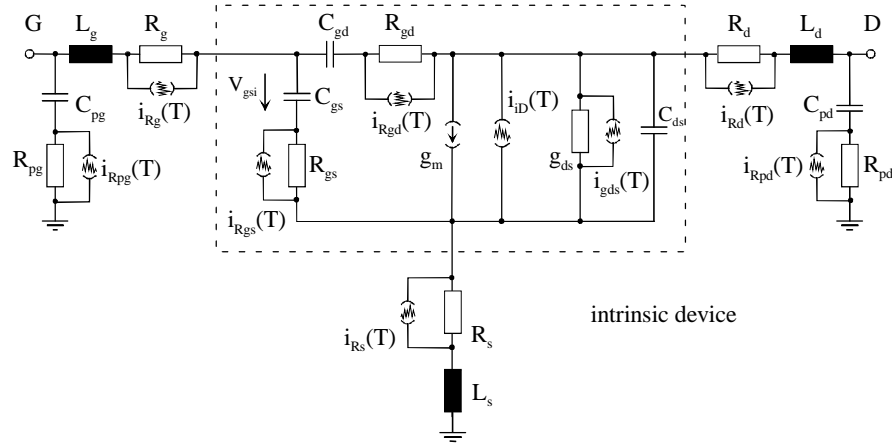


Fig. 2: Noise equivalent circuit model of MOSFET.

The equivalent circuit elements are extracted from measured S parameter data according to the procedure described in [6]. The predictions of the small-signal equivalent circuit agree quite well with the experimental data in the frequency range from 45 MHz to 20 GHz as shown in Fig. 3.

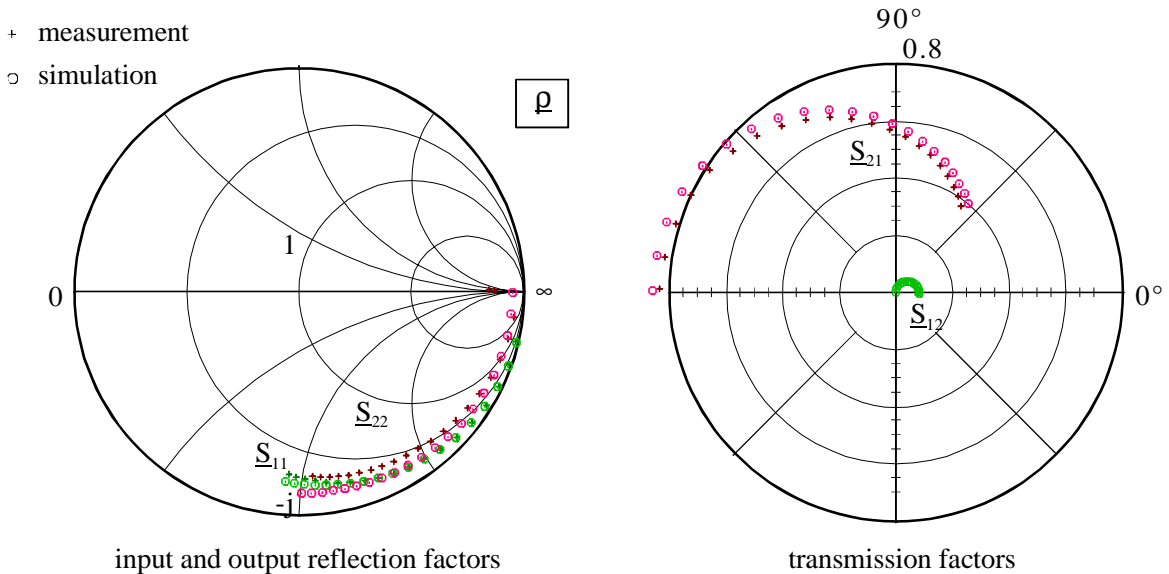


Fig. 3: Comparison between measured S parameter data and those obtained from the model of Fig. 1.

$$V_{ds} = 2 \text{ V}; V_{gs} = 2 \text{ V}; L_g = 0.35 \text{ } \mu\text{m}; W_g = 43.75 \text{ } \mu\text{m}.$$

The noise measurements are performed in the $50 \text{ } \Omega$ environment of the experimental test setup and for model validation also by an automatic noise measurement system with tuned input impedance [7]. The only unknown of the MOSFET noise equivalent circuit is the contribution of the channel current source, which can be obtained as a fitting parameter from a single noise measurement at the operating point or calculated from physical parameters. The comparison of the measured minimum noise figure versus frequency with the calculated data from noise equivalent circuit is shown in Fig. 4. Although the model is too optimistic at lower frequencies, it predicts the optimum source impedance as well as the equivalent noise resistance precisely.

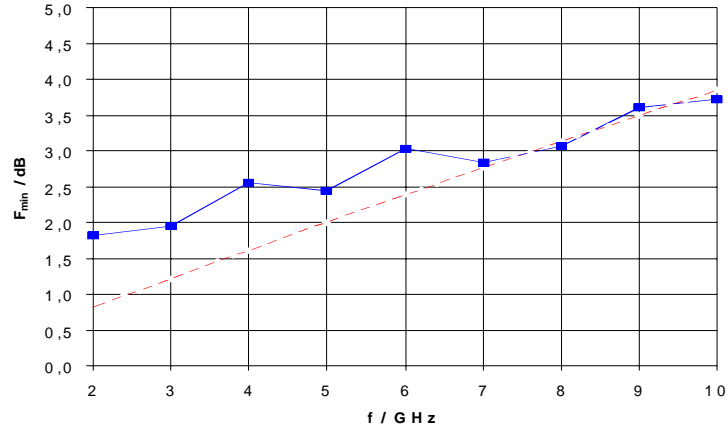


Fig. 4: Measured minimum noise figure versus frequency compared with simulated data of the noise equivalent circuit of the MOSFET.

IV. High Frequency Noise Model of SiGe HBT

Similar to the previous models the intrinsic bipolar transistor is modelled by the Gummel-Poon small-signal equivalent circuit extended by parasitic pad capacitances and series resistances. The substrate losses are described by the resistances in series to the pad capacitances with additional capacitances in parallel as shown in Fig. 5. Again the equivalent circuit elements can be determined from S parameter measurements.

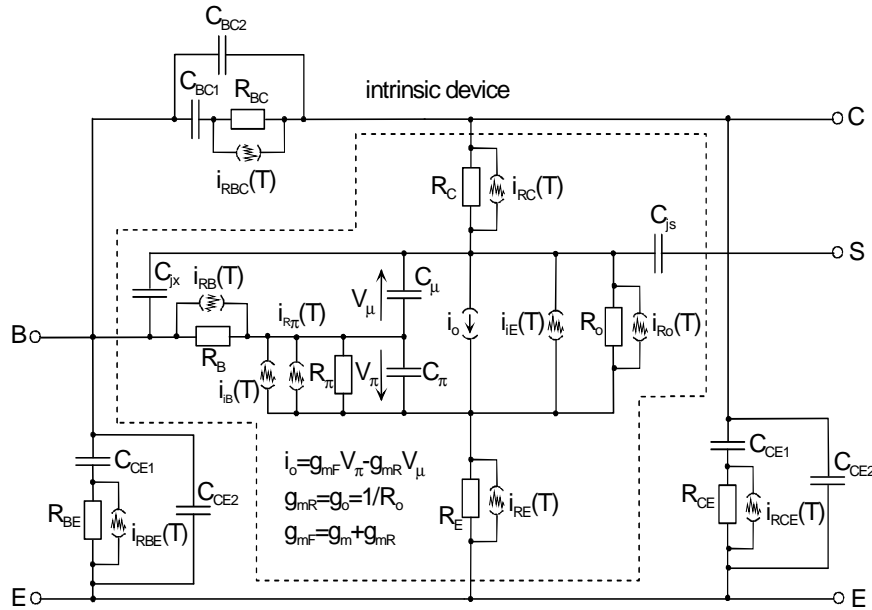


Fig. 5: Noise equivalent circuit of bipolar transistor.

As the bipolar transistor requires a significant base current in the active region the shot noise of the base-to-emitter junction diode has to be considered by an additional noise current source in the intrinsic device model. Again the noise of all resistances of the equivalent circuit are determined by thermal noise, however two current noise sources, $i_{iB}(T)$ and $i_{iE}(T)$, remain unknown and can be calculated as shot noise from the equivalent current sources or obtained as fitting parameters from noise measurements.

Again the noise figures are measured in the 50 Ω environment and for model validation also tuned noise parameter measurements have been performed. One key feature of the noise equivalent circuit models is the ability to identify the noise contribution of each individual noise source for a given operating point at any frequency as shown in Fig. 6. For example below 9 GHz the noise contribution of the base resistance R_B is dominant and thereafter the low pass at the input reduces the signal gain resulting in a larger noise contribution of the output current source.

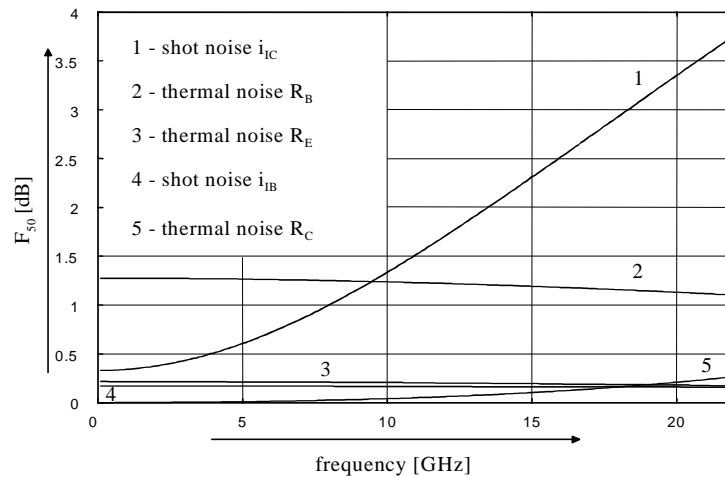


Fig. 6: Noise contributions of the equivalent circuit noise source of the SiGe HBT
 $V_{ce} = 1.6 \text{ V}$; $I_b = 21 \mu\text{A}$; $L = 20 \mu\text{m}$; $W = 1.2 \mu\text{m}$.

V. Discussion

Tuned noise parameter measurements deliver the four noise parameters for each device. However for the design of low noise amplifier accurate high frequency equivalent circuits are a prerequisite which can also be used for the noise modelling. The measured minimum noise figures for the three different devices are shown in Fig. 7 in the frequency range from 2 GHz to 20 GHz. As expected the HEMT is superior to the silicon counterparts in the whole frequency range and the SiGe HBT is superior to the MOSFET. It should be noticed that the transit frequencies of the devices are 120 GHz (HEMT), 45 GHz (HBT) and 18 GHz respectively. The three temperature noise models can easily be adopted with CAD software tools like ADS. The additional information about the individual contributions of each noise source can be used for device optimisation as well as noise property forecasts for future shrunk device geometries.

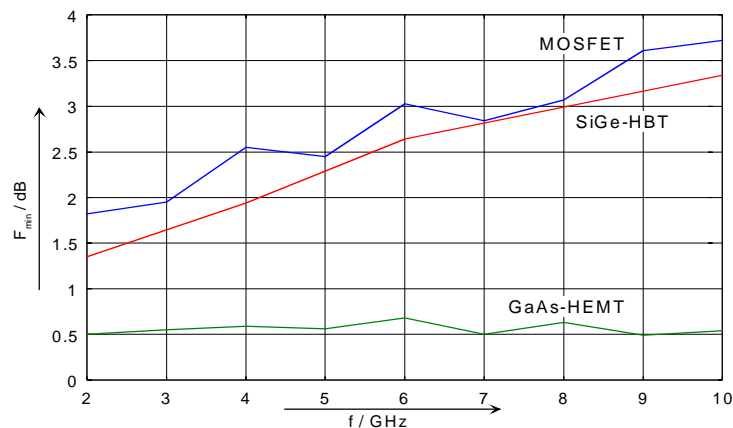


Fig. 7: Minimum noise figure of the different devices.

References:

- [1] A. van der Ziel; Noise in Solid State Device and Circuits, Wiley 1986.
- [2] M.W. Pospieszalski; Modelling of Noise Parameters of MESFET's and MODFET's and their Frequency and Temperature Dependence, IEEE Trans. Microwave Theory and Techn., vol 37, no. 9, 1989, pp. 1340-1350.
- [3] P.J. Tasker, W. Reinert, B. Hughes, J. Braunstein, M. Schlechtweg; Transistor Noise Parameter Extraction Using a 50 Ω Measurement System, IEEE MTT Symp. Digest, Atlanta 1993, pp. 212-216.
- [4] M. Berroth, R. Bosch; High-Frequency Equivalent Circuit of GaAs FET's for Large Signal Applications, IEEE Trans. Microwave Theory and Techn., vol. 39, no. 2, 1991, pp. 224-229.
- [5] G. Dambrine, J.P. Raskin, F. Danneville, D. Vanhoecker-Janier, J.-P. Collinge, A. Cappy; High-Frequency Four Noise Parameters of Silicon-on-Insulator-Based Technology MOSFET for the Design of Low-Noise RF Integrated Circuits, IEEE Trans. Electron Dev., vol. 46, no. 8, 1999, pp. 1733-1741.
- [6] A. Pascht, D. Wiegner, M. Berroth; De-Embedding Procedure for RF Equivalent Circuits of MOSFETs, IEEE MTT workshop Freiburg 1998.
- [7] R. Reuter, Zum Kleinsignal- und Hochfrequenzrauschverhalten von InP-Heterostrukturfeldeffekttransistoren, Shaker-Verlag.